Comparison of EnergyPlus inside surfaces convective heat transfer coefficients algorithms for energy modelling of high-density controlled environment agriculture

Gilbert Larochelle Martin [*], Danielle Monfet

Construction Engineering Department, École de technologie supérieure, Montréal, Canada

ABSTRACT

Energy modelling of high-density controlled environment agriculture (CEA-HD) spaces using a building performance simulation (BPS) tool and a crop energy balance model is emerging as a method to conduct load calculation and energy analysis. However, the modelling hypotheses used in BPS tools have yet to be tailored for CEA-HD spaces and might not be suitable for this specific application. This paper investigates the convective heat transfer coefficient (CHTC) algorithms for inside surfaces included in EnergyPlus to examine their applicability to CEA-HD spaces. The influence of these inside surfaces CHTC algorithms on relevant variables are quantified, with computational fluid dynamics (CFD) computed CHTCs as a reference. The results revealed that certain algorithms (Simple, TARP, and ASTMC1340) are ill-suited to model CEA-HD production spaces compared to CFD-computed reference values. Furthermore, due to the modelled flow rate, the Adaptive Convection algorithm resulted in an aberrant value for the ceiling CHTC. This paper highlights the importance of exercising caution when using BPS tools for energy modelling of CEA-HD spaces.

1. Introduction

Controlled environment agriculture (CEA) involves decoupling crop production from weather variations using an enclosure and an active energy system to optimally control the indoor environment. CEA spaces, including greenhouses, have been extensively studied regarding their thermal modelling [1–3], microclimate spatial variations [4,5], energy systems [6,7], etc. However, since the 2010 s, a new type of CEA production system has been rising: high-density controlled environment agriculture (CEA-HD). CEA-HD, sometimes referred to as vertical farms [8] or plant factories [9], densifies crop production by using multi-tiered hydroponic or aeroponic systems with solely artificial lightning in a low-footprint, highly insulated enclosure. CEA-HD spaces produce high-quality crops, such as leafy greens, lettuce, strawberries, and others, while keeping the produce exempt from pesticides, fungi, or insects at the expense of high energy consumption associated with maintaining optimal indoor conditions [9]. CEA-HD production systems can vary from one another, but Fig. 1 provides an example of an industrial-scale CEA-HD production space.

The indoor conditions within these production spaces vary from one crop to another and may not remain constant throughout the production cycle. Adjustments are implemented to promote crop growth and control diseases according to the growing stage and other influential factors. The indoor conditions of a CEA-HD space can be described using the airflow speed, the vapour pressure deficit (VPD), the carbon dioxide concentration and the photosynthetically active radiation (PAR) levels. The VPD represents the potential for evaporation at the leaf level and is computed by combining the indoor air temperature and humidity content [11]. The PAR is the electromagnetic radiation between 400 and 700 nm [12] necessary for the crop's photosynthesis. Indoor conditions setpoints and control strategies directly impact the energy use and peak demand of CEA-HD spaces, which are closely related to their financial viability. Still, little is published on those production spaces' best design and operating practices, as most of the knowledge is proprietary [13]. Furthermore, the various aspects of CEA-HD [7,14,15] represent an ongoing area of research, given the current need for growers, engineers, utilities and policymakers to assess them.

To tackle this issue, CEA-HD energy models have been proposed in the literature [16,17]. These models are often problem-specific, not flexible enough for broad usage and not necessarily publicly available. As such, developing CEA-HD models using more holistic modelling tools is essential. Building performance simulation (BPS) modelling tools can

---

Fig. 1. Example of an industrial-scale CEA-HD production space [10].

Fig. 2. Schematic of the EnergyPlus heat balance method on a thermal zone [26].

Table 1
Variables used by the EnergyPlus CHTCs algorithms.

Algorithm	Variables	Details
Simple	Constant	Developed for natural convection cases.
TARP	$f(\Delta T, \theta)$	Only surface tilt angle and temperature considered.
Ceiling Diffuser	$f(ACH)$	Developed for an isothermal room with a cold ceiling jet.
Adaptive Convection	$f(\Delta T, \theta, ACH, D_h, H, T_{si}, T_{SA}, Ra, k, \dot{V}, L)$	Assumption for airflow inlet/outlet position and orientation might not apply.
ASTMC1340	$f(Gr, Pr, Ra, Re, \theta, k, L)$	Developed for attic space.

models.

In BPS tools, the energy exchanges are often modelled using the heat balance approach [25]. Fig. 2 illustrates the different energy exchanges considered in the heat balance algorithm of EnergyPlus [21]. The air heat balance within the thermal zone is determined using the convection heat transfer between the internal surfaces and the zone air. The modelled heating, ventilation and air conditioning (HVAC) system subsequently adds or removes energy from the thermal zone to meet its specified setpoint, i.e., the specified indoor air conditions to be maintained.

The convection heat transfer to the zone air (q_{conv}) is defined according to equation (1), where the convective heat transfer coefficient (CHTC) for each surface (h_{ci}) can be modelled according to different approaches [35]. The convection heat transfer to the zone air is computed using the surface area (A_i), the interior surface temperature (T_{si}) and the zone air temperature (T_a).

$$q_{conv} = \sum_{i=1}^{n} A_i \cdot h_{ci} \hat{A} \cdot (T_{si_i} - T_a) \tag{1}$$

In CEA-HD spaces, the inside surface boundary conditions are not representative of typical building space since the internal sensible and latent heat gains associated with crop transpiration are high [18]. Thus, HVAC systems used in these production spaces are set to higher airflow rates to promote indoor environment uniformity and crop transpiration. Hence, the CHTC for each inside surface differs from conventional building spaces and the CHTC algorithms used in BPS tools might not be suitable for CEA-HD modelling.

In EnergyPlus, five options are available for calculating the CHTC for inside surfaces: Simple, TARP, Ceiling Diffuser, Adaptive Convection and ASTMC1340 algorithms. The choice of algorithm to use can vary according to the surface orientations, room airflow conditions, and heat flow direction. The Simple algorithm specifies a fixed CHTC value associated with natural convection for each room surface. The TARP algorithm, the default choice in EnergyPlus, is a natural convection model that correlates the CHTC to the surface orientation and the temperature difference between the zone air and the selected surface. These correlations are no longer available in the American Society of Heating and Air-Conditioning Engineers (ASHRAE) Handbook of Fundamentals [26]. Both the Simple and TARP algorithms are based on the work of Walton [27]. The Ceiling Diffuser algorithm, based on the experiments of Fisher and Pedersen [28], uses correlation based on the air change per hour (ACH) to predict the CHTC of the inside surfaces. The Adaptive Convection algorithm, developed by Beausoleil-Morrison [29], is a more general algorithm that selects specific correlations based on the flow regime and the room configuration. It leverages the work of Alamdari and Hammond [30], Khalifa [31], Awbi and Hatton [32] and Fisher [33], supplemented by mixed convection correlations obtained with blending techniques. The ASTMC1340 algorithm, developed for attic energy models, is based on the technical document of the same name [34] and was implemented in EnergyPlus by Fontanini, Castro Aguilar, Mitchell, Kosny, Merket, DeGraw and Lee [35]. A recent review by Camci, Karakoyun, Acikgoz and Dalkilic [36] summarised the correlations for different flow types (i.e., natural convection, forced
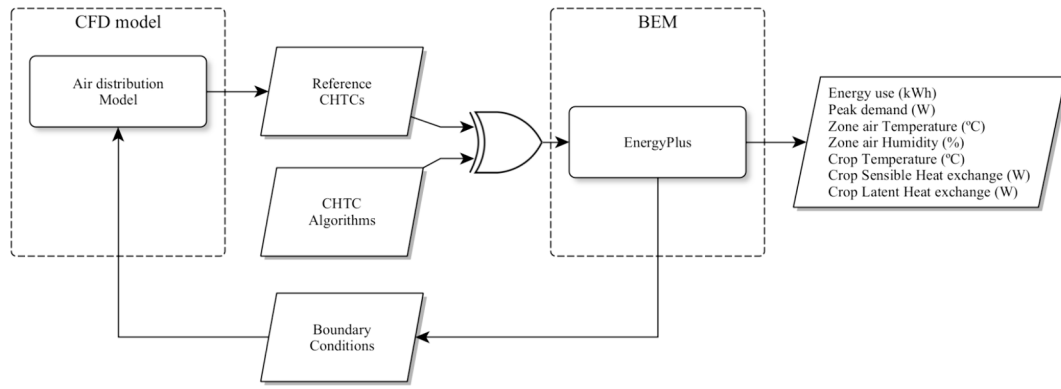
help analyse the thermal exchanges through the enclosure, energy systems, and associated controls. Recently, a heat balance model at the crop leaf level has been integrated into a building performance simulation (BPS) tool [18] and adapted for its use in EnergyPlus. This integration is leveraging substantial ongoing research from the building performance simulation (BPS) field. BPS tools [19–23] have been used for decades to inform architects and engineers on multiple aspects of building design, optimisation and operation. Indeed, these tools can be used to perform several types of analysis, such as predicting buildings' thermal loads and assessing energy performance, energy efficiency, demand response measures, etc. [24]. Furthermore, they have been designed to consider multiple building configurations and buildings' energy exchange processes. Using BPS tools to model CEA-HD production spaces could address most of the shortcomings of the previously published CEA-HD

Fig. 3. Overview of the proposed methodology.

convection, mixed convection) developed for indoor applications. An overview of the variables used by the EnergyPlus inside surfaces CHTCs algorithms is presented in Table 1, where ΔT is the temperature difference between the interior surface and the thermal zone air temperature, θ is the surface tilt angle, ACH is the zone air changes per hour, D_h is the hydraulic diameter, H is the characteristic height, L is the characteristic length, T_{si} is the surface temperature, T_{SA} is the supply air temperature, Ra is the Rayleigh number, k is the air thermal conductivity, Gr is the Grashof number, Pr is the Prandtl number, and Re is the Reynolds number.

The choice of CHTC to be used is not trivial [37]. Indeed, choosing a specific type of correlation over another can impact the building's peak heating demand by up to 30.5 % and peak cooling demand by up to 55.2 % [38]. Differences also exist between correlations obtained from comparable experiments as they are derived from a single geometry [39]. To the authors' knowledge, the algorithm or values used for computing the CHTC for inside surfaces in CEA-HD spaces using BPS tools are often not specified.

Hence, this paper aims to identify which internal surface CHTC algorithm available in the BPS tool EnergyPlus is more appropriate to model CEA-HD spaces. It also seeks to provide reference values based on computational fluid dynamics (CFD). The impact of selecting an inappropriate algorithm is also quantified using a small-scale CEA-HD production space case study.

2. Methodology

The proposed method compares different inside surfaces CHTC algorithms available in EnergyPlus with reference CHTC values computed using CFD. The five options available in EnergyPlus (Simple, TARP, Ceiling Diffuser, Adaptive Convection and ASTMC1340) are used in a case study to assess their influence on energy use and peak demand, as well as air conditions and critical aspects of crop modelling. The case study leverages two different models: (1) a computational fluid dynamics (CFD) model and (2) a building energy model (BEM), as illustrated in Fig. 3. In summary, the ANSYS Fluent R19.2 CFD air distribution model, with boundary conditions extracted from the EnergyPlus BEM, was used to generate the reference CHTCs. In EnergyPlus, the CHTC values can be defined by the users, for example, by specifying the computed CHTC for each surface using the CFD model or by selecting one of the algorithms listed in Table 1. Simulation results are generated for all cases. The small-scale CEA-HD production space, the CFD model and the BEM are described in the following sections.

The CHTC reference values are obtained through CFD modelling of the space, including the impact of crops. Indeed, CFD has already been used to develop natural convection Nusselt number correlations for building rooms [40,41]. This provides a Navier-Stokes based reference tailored to the specific configuration of the small-scale CEA-HD space since in forced convection applications, the correlation used should
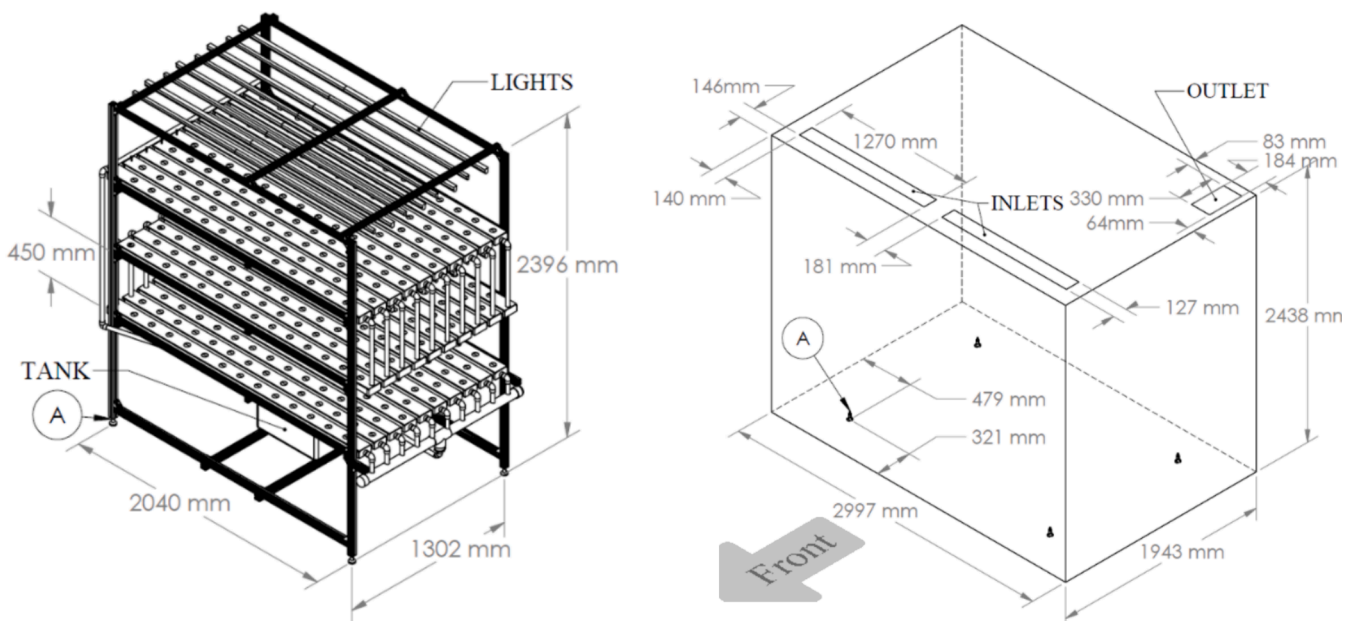

Fig. 4. Isometric view of the hydroponic production system (left) and production space enclosure (right).
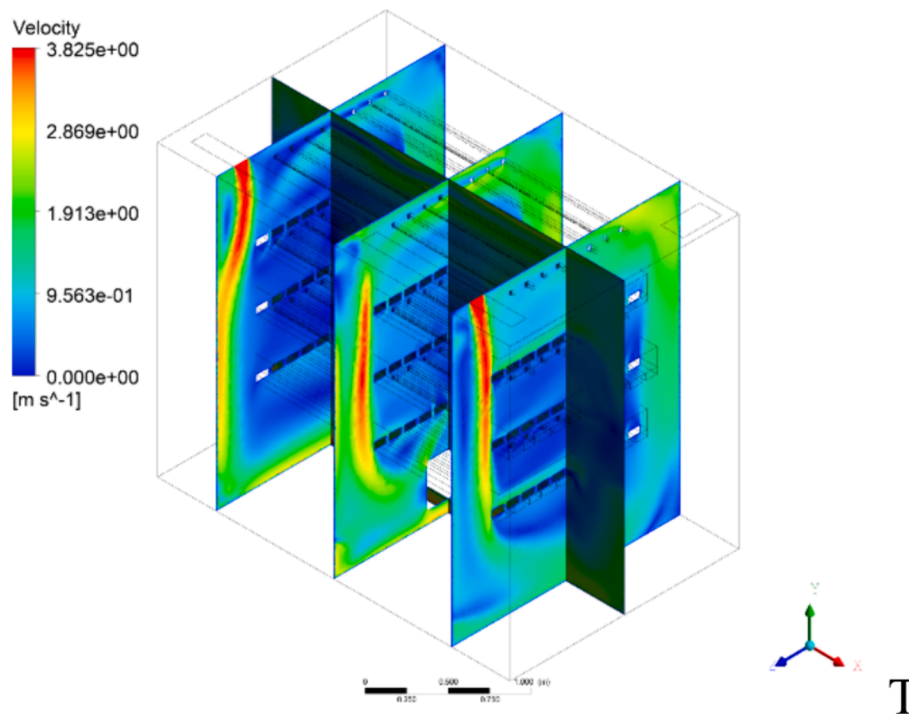
Fig. 5. Velocity magnitude results for the CFD model [44].

account for the airflow rate and the locations of the inlet/outlet [36]. The influence of the different CHTC values and algorithms on the energy use and peak demand and the thermal zone air temperature, air humidity, crop temperature, and crop sensible and latent heat exchanges between the crops and the zone are also quantified and compared.

2.1. Small-scale CEA-HD production space

The CEA-HD production space used as a case study is a small-scale hydroponic lettuce production system, as illustrated in Fig. 4. The production space enclosure walls are made of highly insulated thermal structural panels having a thermal conductance value of 0.12 W·(K·m²)⁻¹, a thermal capacity of 100 J·(kg·K)⁻¹, and a density of 113.17 kg·m⁻³. The temperature and relative humidity setpoints are 21 °C/70 % during the photoperiod, from 4 h00 to 22 h00 (18 h), and 18 °C/74 % during the dark period. The light emitting diode (LED) lamps are designed with a power density of 144.23 W·m⁻² of cultivated area and a photosynthetic photon flux density (PPFD) of 288.5 μmol·s⁻¹·m⁻² and a visible fraction of 0.52. The same lighting power density was used in the CFD and building energy model. The LAI, defined by the total one-sided leaf area per horizontal surface unit [42], is specified as 1 and the crop reflectivity as 5 % for both models. The production enclosure is located in a conditioned research laboratory with controlled temperature and humidity. The location of the air distribution system inlets and outlet are shown in Fig. 4, including the production space and system dimensions.

2.2. CFD model

A computational fluid dynamics (CFD) model of the air distribution of the CEA-HD space illustrated in Fig. 4 was previously developed in ANSYS Fluent R19.2 using the k-ε turbulence model [43] and user-defined functions (UDFs) to account for the crop airflow impingement, photosynthesis, and sensible and latent heat exchanges [44]. In the UDFs, it was assumed that the only source of water vapour was the transpiration from the crops since the evaporation of the nutritive solution can be assumed to be negligible in enclosed hydroponic systems [45]. These UDFs solve the heat balance at the leaf level in each cell

using a numerical root-finding algorithm (secant method) and add a CO_2 sink. CFD crop modelling uses numerical schemes (the semi-implicit method for pressure-linked equations (SIMPLE) [46] in this case) to solve the Navier-Stokes, energy and mass transport equations in the specified spatial domain. A grid convergence analysis showed no variation in the average relative humidity and average airflow speed inside the porous media zone, the crop zone, of the lower growing tier with regard to the number of cells of the CFD model. The mesh cell growth rate used for the enclosure surfaces inflation layer was 1.35, resulting in an average grid skewness of 0.20. The boundary conditions of the modelled domain need to be specified in the CFD tool (Fluent 19.2). These are specified using results from the building energy model (BEM) using the EnergyPlus default CHTC algorithm (TARP algorithm), as illustrated in Fig. 3. The BEM estimates the temperature of the inside surfaces according to the heat balance method of the thermal zone. Subsequently, using a reference bulk fluid temperature, the CFD model can be used to compute the average CHTC for each internal surface. The CHTC values computed with the CFD model are then used as inputs for the energy model. The BEM is then used to conduct a yearly simulation for the analysis (see Fig. 3).

The CFD model needs to resolve the boundary layer of each enclosure surface using a high-resolution mesh to stay well within the viscous sublayer and, thus, properly evaluate the temperature gradient at the boundary. The CFD model was developed using the standard wall functions, which apply the laminar stress–strain relationship at values of y* below 11.225 (in the context of the presented case study y+≈y*). The dimensionless wall distance (y^+) value used in the CFD model is approximately one for all the enclosure surfaces in the CFD model to stay well within the linear viscous sub-layer of the boundary layer [47]. The dimensionless wall distance is detailed in equation (2) where y^+ is the dimensionless wall distance, ρ is the fluid density (kg·m⁻³), τ_w is the wall shear stress (Pa) and μ is the fluid dynamic viscosity (Pa·s). The velocity magnitude results of the CFD airflow simulation in the CEA-HD production space on selected planes are presented in Fig. 5. Further CFD model results are shown in [44].

Table 2

Computed inside surfaces CHTC values using computational fluid dynamics (CFD) and the EnergyPlus inside convection algorithms.

Surface	CFD	E + Simple	E + TARP		E + Ceiling Diffuser	E + Adaptive Convection	E + ASTMC1340	
			21 °C/70 %	18 °C/74 %			21 °C/70 %	18 °C/74 %
Front	41.61	3.07	3.34	0.77	17.55	43.09	2.79	1.5
Right	24.62	3.07	3.34	0.77	17.55	43.04	2.79	1.5
Back	29.82	3.07	3.34	0.77	17.55	43.09	2.79	1.5
Left	34.54	3.07	3.34	0.77	17.55	43.04	2.79	1.5
Ceiling	34.42	0.95	1.96	0.45	43.80	3.44e + 06	1.58	1.5
Floor	38.95	4.04	3.86	0.87	11.35	28.93	4.03	1.6

N.B. values are given in W·m^{-2}·K^{-1}.

$$y^+ = \frac{\rho y \left(\sqrt{\frac{\tau_w}{\rho}} \right)}{\mu} \qquad (2)$$

Post-treatment of the CFD results is necessary to extract the average boundary surface CHTC. The CFD reference CHTC values are thus derived from the temperature field results as the surface heat flux at the boundary using equation (3). The temperature gradient over a boundary adjacent cell yields the total heat flux for this cell, and by averaging these values, the mean CHTC for the boundary surfaces is obtained. Equation (3) describes the heat flux evaluated at the domain boundary using Fourier's law, and equation (4) represents the average surface CHTC using a reference bulk temperature (21 °C) where q_s is the surface adjacent cell heat flux (W·m^{-2}), $\overline{q_s}$ is the surface average heat flux (W·m^{-2}), k is the thermal conductivity of the fluid (W·m^{-1}·K^{-1}), T is the temperature (K), y is the absolute distance from the wall (m), h_c is the average surface heat transfer coefficient (W·m^{-2}·K^{-1}), T_{si} is the surface temperature (K) and T_a is the zone air temperature (K).

$$q_s = k \frac{\partial T}{\partial y} \bigg|_{y=0} \qquad (3)$$

$$h_c = \frac{\overline{q_s}}{(T_{si} - T_a)} \qquad (4)$$

2.3. Building energy model

The building energy model of the experimental CEA-HD production space was developed using the internal gains described in the production space section. The sensible and latent loads of the production space were computed using the EnergyPlus ideal load option.

A crop energy balance model, developed by Talbot and Monfet [18] based on the steady-state lettuce crop model proposed by Graamans, van den Dobbelsteen, Meinen and Stanghellini [16], was adapted and added to the energy model using the EnergyPlus Python API. The proposed model was programmed to represent the original Fortran-based TRNSYS type as closely as possible. However, the algorithm solver was modified to improve code performance. As such, a fixed-point iteration algorithm was used to solve the energy balance equation rather than the super-linear secant method, implemented in the original TRNSYS version of the model, for which convergence was not guaranteed. The implementation was verified by comparing the obtained results for the computed leaf surface temperature and the gains/losses calculated using the developed model. The residuals between the leaf temperature simulated in TRNSYS and EnergyPlus were 0.14 °C for the maximum absolute difference (MAD) and 0.038 °C for the root mean square error (RMSE). The comparison of the computed heat gain/loss from the crop energy balance model in TRNSYS versus EnergyPlus led to a normalised mean bias error (NMBE) of less than 0.06 % for both the convective (sensible) heat gain/loss and latent in heat gain from crops.

To account for the CFD model flow conditions over an entire year, the EnergyPlus simulation was carried out with a fixed supply airflow rate using an energy management system (EMS) program. This limitation of the proposed method is caused by the high computing power required to perform a strong coupling between the CFD model and the BEM for yearly simulation. Since the supply airflow rate is fixed, the underlying hypothesis is that the computed CFD-computed CHTC values remain constant throughout the year. The building energy model
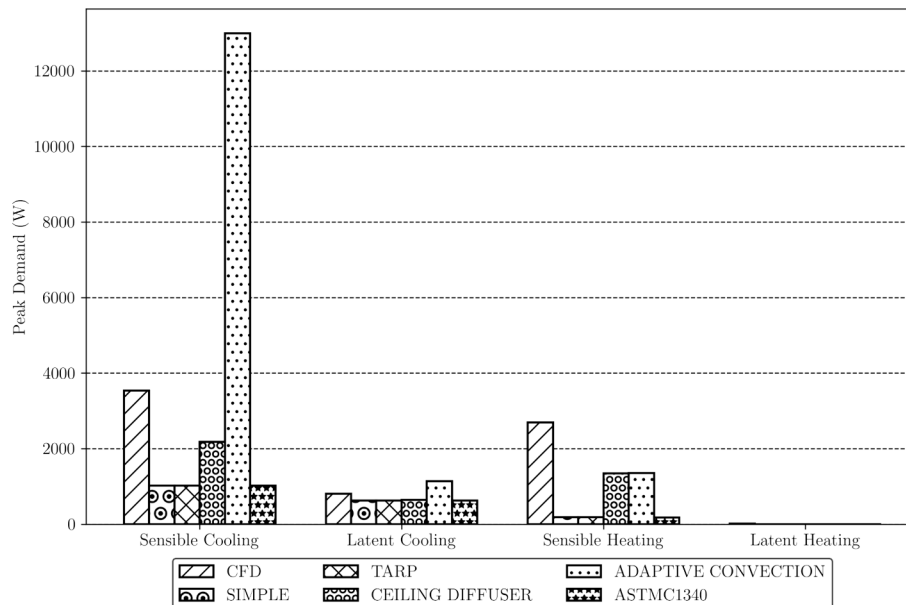
Fig. 6. Yearly peak demand comparison by end-uses between the different CHTC algorithms.
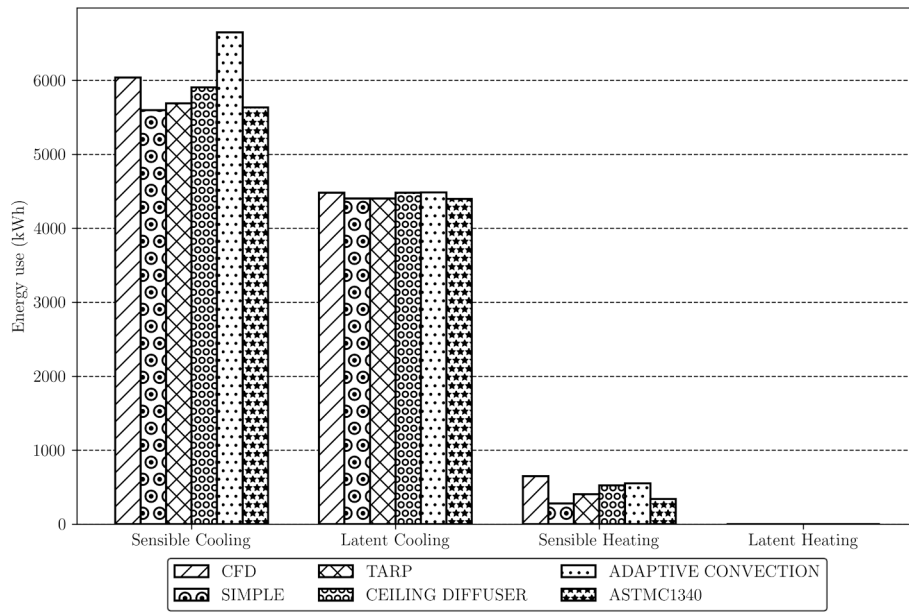
Fig. 7. Yearly energy end-use comparison between the different CHTC algorithms.
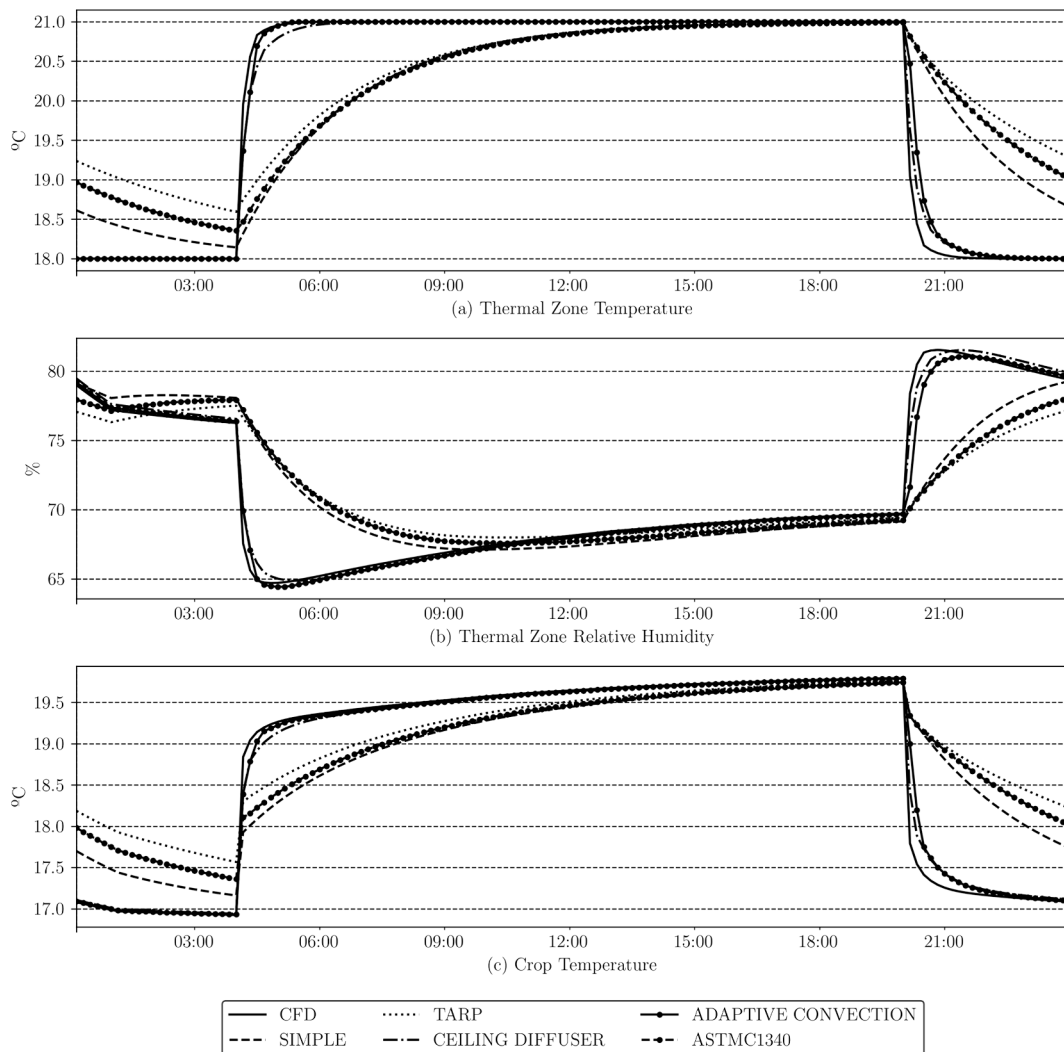

Fig. 8. Typical day CEA-HD energy model (a) zone air temperature, (b) relative humidity and (c) crop temperature.
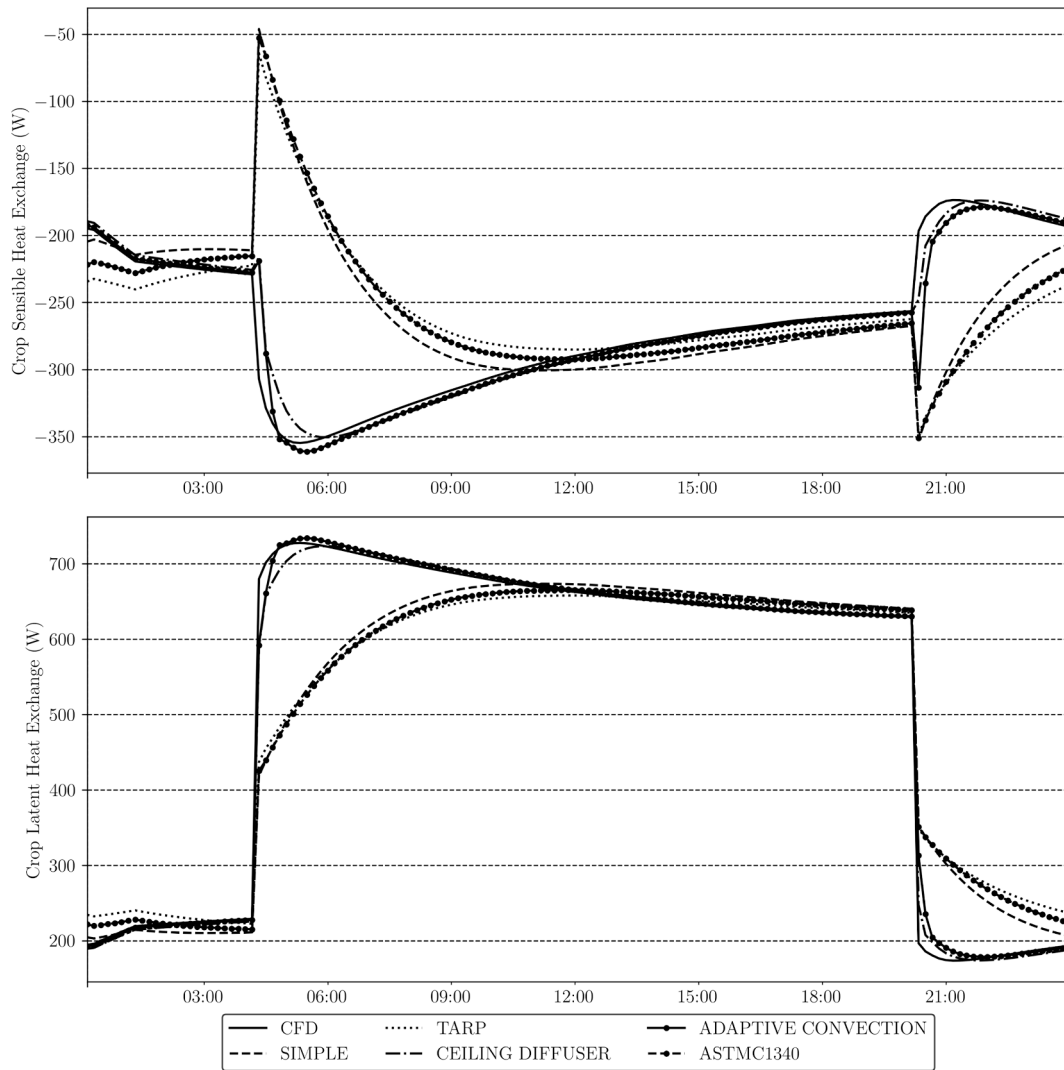
Fig. 9. Crop sensible and latent heat exchanges between the crops and the zone air computed by the building energy model for a typical day.

consists of a single thermal zone with a fixed supply airflow rate and does not explicitly model the HVAC system. Given the multiple options available to model the heat conduction through the enclosure in EnergyPlus, the default option (conduction transfer functions) was used for the simulation. The outside boundary conditions of all the enclosure surfaces were set to a constant temperature of 20 °C and a combined convective-radiative film coefficient of 17.8 W·m^{-2}·K^{-1} with no sun or wind exposure to represent the environment of the conditioned research laboratory where the CEA-HD production space is located.

3. Results

The CHTC values computed by EnergyPlus are compared against CFD reference CHTC values to assess the variation between the different algorithms. Table 2 compiles the CHTC values for each of the six surfaces of the production space enclosure computed with CFD, Simple, TARP, Ceiling Diffuser, Adaptive Convection and ASTMC1340 algorithms. The surfaces are referenced according to the orientation presented in Fig. 4. Upon examination of the values of Table 2, it is evident that the values computed with the Adaptive Convection algorithm are approximately within the same order of magnitude as the CFD reference values, albeit at the expense of a notably aberrant ceiling CHTC. Indeed, the forced convection flow regime in gases is expected to yield a CHTC between 25 and 250 W·m^{-2}·K^{-1} [26]. The source of this issue for the ceiling CHTC

could not be identified, but it seems to be linked to the Fisher-Pedersen ceiling diffuser correlation when a setpoint change occurs. It is unclear if the issue stemmed from the adaptive convection algorithm itself or from a combination of the modelling method (using ideal loads with fixed EMS airflow) and the algorithm. The other EnergyPlus algorithms computed lower inside surfaces CHTCs than the CFD reference values, except for the Ceiling Diffuser algorithm ceiling surface. This difference can be explained by the orientation of the supply air inlet jet (see Fig. 5).

The impact of the different CHTC algorithms on the production space energy use and peak demand is presented in Fig. 6 and Fig. 7, respectively. The difference in the computed CHTC values has a more significant impact on the peak demand than energy use. For example, the estimated sensible peak demand varies between 1 kW and 13 kW, while the estimated sensible cooling energy use varies between 5500 kWh and 6500 kWh. The sensible cooling peak demand for the Adaptive Convection algorithm is significantly higher, linked to the aberrant value of the ceiling CHTC shown in Table 2.

The impact of the different computed CHTC values was then assessed on the daily profiles of critical CEA-HD variables, such as the zone air temperature, relative humidity, and crop temperature, as presented in Fig. 8. These variables are critical for solving the heat balance at the crop level, resulting in the computation of sensible and latent heat exchanges between the crops and the zone. Fig. 8 shows two emerging clusters: (1) the Simple, TARP, and ASTMC1340 algorithms and (2) the Ceiling
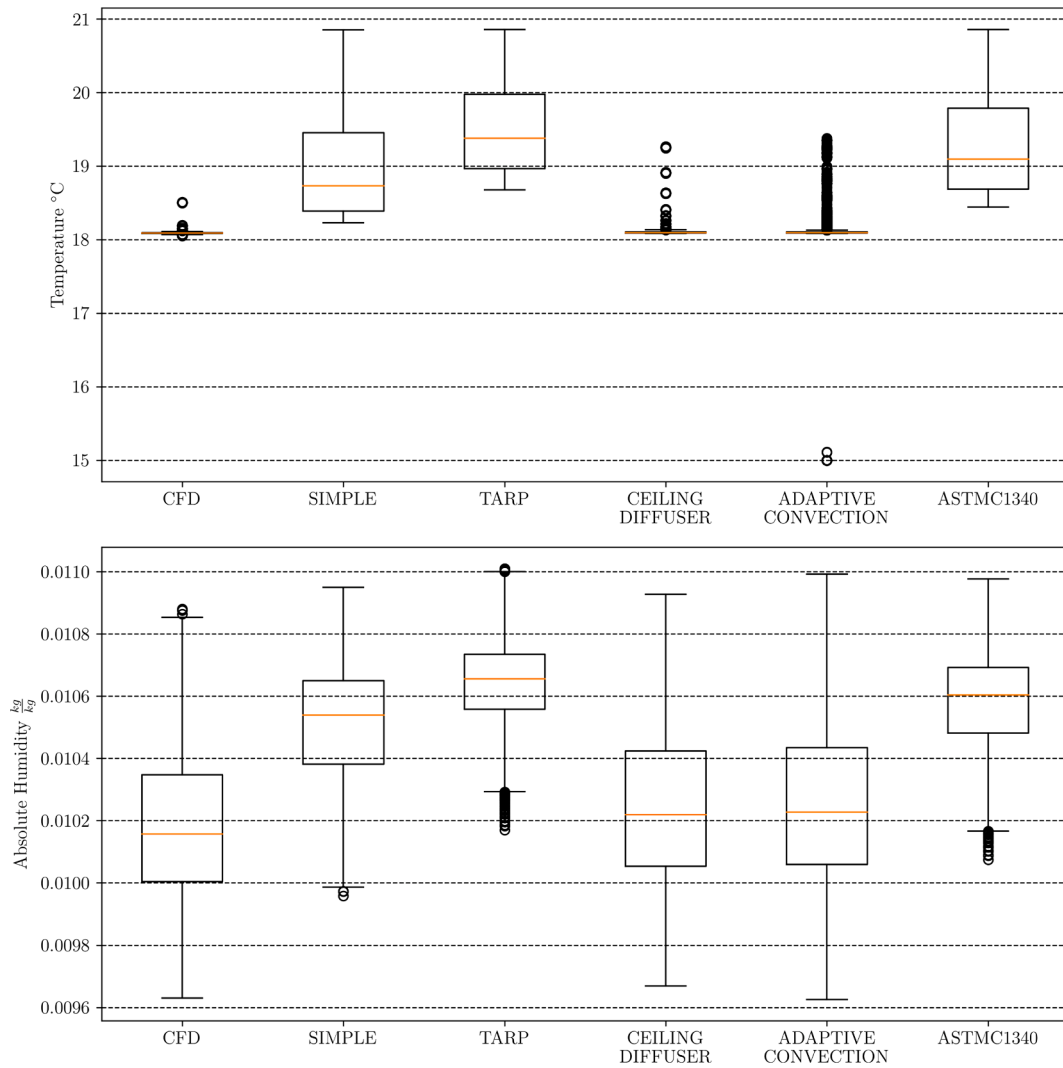
Fig. 10. Yearly supply inlet temperature and absolute humidity results computed by the BEM.

Diffuser, Adaptive Convection, and CFD-derived CHTC values. This suggests that the Simple, TARP, and ASTMC1340 algorithms might be ill-suited for modelling CEA-HD spaces based on the CFD computed CHTC values.

The crop sensible and latent heat exchanges between the crops and the building zone air, both outputs of the leaf level heat balance, are presented for a typical production day in Fig. 9. The same two clusters identified in Fig. 8 are observed in Fig. 9. These further support disregarding the Simple, TARP, and ASTMC1340 algorithms for BEM of CEA-HD spaces. The peak crop cooling effect (negative crop sensible heat exchange) is underestimated at the beginning of the photoperiod by a factor of 5 for the ill-suited cluster of algorithms. Fig. 9 also partly explains why the impact is higher on the peak demand than energy use. Indeed, the absolute discrepancies between the curves of Fig. 9 impacting peak demand are more pronounced than the difference in area under the different curves associated with energy use.

To meet the load requirement, the zone supply air temperature and absolute humidity fluctuated as the supply airflow rate remained fixed. The zone supply air inlet temperature and absolute humidity computed using the energy model also vary from one CHTC algorithm to another. Fig. 10 illustrates the distribution of those two supply air variables over a yearly simulation for each inside surface CHTC algorithm. The previously identified ill-suited algorithm cluster exhibits a broader range in supply inlet temperatures with a narrower range in relative humidity. This becomes particularly relevant when using the energy model for

HVAC control sequence development or performance evaluation. Indeed, using an inappropriate CHTC algorithm might yield suboptimal, inadequate rule-based control sequences and potentially adversely affect the production microclimate.

4. Discussion

The results presented in this paper highlight the discrepancies in peak demand, energy use, thermal zone temperature, humidity, crop temperature and the sensible and latent heat exchanges between the crops and the zone air that can be caused by an ill-advised selection of the inside surface CHTC algorithm in CEA-HD spaces energy modelling using the BPS program EnergyPlus. While CHTC values directly impact the BPS computed results, further exploration of the different assumptions used in BPS tools, such as EnergyPlus, must be performed before the widespread use of BPS for CEA-HD energy modelling. Indeed, other algorithms used for wall conduction or radiation exchanges, for example, could result in discrepancies for additional critical heat or mass transfer. Concerningly, recent research using BPS for CEA-HD energy modelling is often performed by authors outside the BPS field, leading to oversimplification of the building energy model used.

One limitation of the performed analysis is that the boundary conditions of the CFD model should ideally be dynamic and not fixed. Hence, the temperature used for the surfaces of the CFD model should vary using the results of a heat balance calculation in the thermal zone of

the building energy model. Ideally, convergence between the two tools would be reached for each timestep of a yearly simulation run period. This is still very challenging, given the currently available computing power. Coupling the CFD and BEM could enhance the methodology used when advances in CFD modelling and/or computing power are made. Furthermore, particular attention to the mesh size and the governing equations is critical. As the wall adjacent mesh y + has to be below 5 to stay within the viscous sublayer region of the boundary layer, the mesh quality becomes a critical factor impacting solution convergence. Indeed, model cell count must be increased to keep an acceptable cell aspect ratio at the boundary faces as cell sizing is reduced. Maintaining mesh quality with the small inflation layer needed at the mesh boundaries to keep an acceptable y + value is challenging.

Fixing the supply airflow rate during the energy model simulation simplifies the real production space operating conditions. Indeed, the required airflow rate might vary depending on several factors such as lighting schedule, crop growing stage, sensible heat ratio, etc. Using a single CFD computed reference CHTC value for the year is a limitation of this paper that could be addressed in the future by extracting correlations from multiple CFD modelled production space operating conditions. Furthermore, the issue with the ceiling CHTC raised questions about using the adaptive convection algorithm under specific operating conditions, which could be addressed in future EnergyPlus releases by limiting the range of possible output values.

One major limitation of the proposed work is the lack of real-world measurements. As advanced as CFD models may currently be, measurements are still a critical requirement for validation. CHTC measurements are costly and complex, yet they may provide further insights into developing more precise CEA-HD inside surfaces, CHTC correlations or algorithms, or algorithm modification. Perhaps a more manageable alternative would be to validate the energy model given access to operating CEA-HD production spaces. Access to this data type is challenging as producers frequently hesitate to share information closely tied to their financial and production performance. After extensive validation, the results from the energy model offer a wide range of practical applications, including assessing the energy impacts under various production space operating conditions, enclosure compositions, HVAC control sequences, etc. This can support the development of guidelines and design tools for HVAC engineers and production space designers based on validated models.

5. Conclusion

This paper investigates the impact of inside surfaces convection heat transfer coefficient (CHTC) on energy metrics for a small experimental high-density controlled environment agriculture (CEA-HD) production space. The analysis used the EnergyPlus building performance simulation (BPS) tool, computational fluid dynamics (CFD) and crop modelling. The results showed that specific algorithms packaged with EnergyPlus (Simple, TARP, and ASTMC1340 algorithms) are ill-suited to model CEA-HD production spaces based on CFD computed reference values. Furthermore, none of the investigated algorithms proved perfectly suited to the simulation outputs obtained using CFD reference values. While some algorithms produced closer simulation results for critical CEA-HD variables (such as zone air temperature, relative humidity, crop temperature, crop sensible and latent heat exchanges), they still exhibited discrepancies in the computed yearly peak demand and energy end-use distribution. This paper aims to serve as a foundation for comprehensive research on energy modelling of CEA-HD production spaces using BPS tools.

CRediT authorship contribution statement

Gilbert Larochelle Martin: Writing – review & editing, Writing – original draft, Visualization, Methodology, Investigation, Formal analysis, Conceptualization. **Danielle Monfet:** Writing – review & editing,

Supervision.

Declaration of competing interest

The authors declare that they have no known competing financial interests or personal relationships that could have appeared to influence the work reported in this paper.

Data availability

Data will be made available on request.

References

[1] J.G. Pieters, J.M. Deltour, Modelling solar energy input in greenhouses, Sol. Energy 67 (1–3) (1999) 119–130.

[2] J.C. Roy, T. Boulard, C. Kittas, S. Wang, Convective and ventilation transfers in greenhouses, part 1: The greenhouse considered as a perfectly stirred tank, Biosyst. Eng. 83 (1) (2002) 1–20.

[3] D. Katzin, E.J. van Henten, S. van Mourik, Process-based greenhouse climate models: Genealogy, current status, and future directions, Agr. Syst. 198 (2022) 103388.

[4] T. Boulard, J.-C. Roy, J.-B. Pouillard, H. Fatnassi, A. Grisey, Modelling of micrometeorology, canopy transpiration and photosynthesis in a closed greenhouse using computational fluid dynamics, Biosyst. Eng. 158 (2017) 110–133.

[5] T. Boulard, C. Kittas, J.C. Roy, S. Wang, SE—Structures and environment: convective and ventilation transfers in greenhouses, Part 2: Determination of the distributed greenhouse climate, Biosyst. Eng. 83 (2) (2002) 129–147.

[6] A. Vadiee, V. Martin, Energy management in horticultural applications through the closed greenhouse concept, state of the art, Renew. Sustain. Energy Rev. 16 (7) (2012) 5087–5100.

[7] N. Engler, M. Krarti, Review of energy efficiency in controlled environment agriculture, Renew. Sustain. Energy Rev. 141 (2021) 110786.

[8] D. Despommier, The Vertical Farm: Feeding The World in the 21st Century, Macmillan, 2010.

[9] T. Kozai, G. Niu, M. Takagaki, Plant Factory: An Indoor Vertical Farming System for Efficient Quality Food Production, Academic press, 2019.

[10] AeroFarms (Accessed January 24th 2024). About AeroFarms The Vertical Farming, Elevated Flavor Company. https://www.aerofarms.com/about-us/.

[11] W. Fricke, Water transport and energy, Plant Cell Environ. 40 (6) (2017) 977–994.

[12] K.J. McCree, The action spectrum, absorptance and quantum yield of photosynthesis in crop plants, Agric. Meteorol. 9 (1971) 191–216.

[13] D.L. Jonlin, D.J. Lewellen, A low-energy high managing energy use for commercial indoor cannabis cultivation, Energy Eng. 114 (4) (2017) 69–79.

[14] F. Kalantari, O.M. Tahir, R.A. Joni, E. Fatemi, Opportunities and challenges in sustainability of vertical farming: A review, J. Landscape Ecol. 11 (1) (2018) 35–60.

[15] K. Al-Kodmany, The vertical farm: A review of developments and implications for the vertical city, Buildings 8 (2) (2018) 24.

[16] L. Graamans, A. van den Dobbelsteen, E. Meinen, C. Stanghellini, Plant factories; crop transpiration and energy balance, Agr. Syst. 153 (2017) 138–147.

[17] T. Weidner, A. Yang, M.W. Hamm, Energy optimisation of plant factories and greenhouses for different climatic conditions, Energ. Conver. Manage. 243 (2021) 114336.

[18] M.-H. Talbot, D. Monfet, Estimating the impact of crops on peak loads of a Building-Integrated Agriculture space, Sci. Technol. Built Environ. 26 (10) (2020) 1448–1460.

[19] L. University of Wisconsin-Madison, Solar Energy, TRNSYS, a transient simulation program, The Laboratory, Madison, Wis, 1975, 1975..

[20] B. Birdsall, W. Buhl, K. Ellington, A. Erdem, F. Winkelmann, Overview of the DOE-2 Building Energy Analysis Program, Report LBL-19735m rev. w, Lawrence Berkeley Laboratory, Berkeley, CA, 1990.

[21] D.B. Crawley, L.K. Lawrie, F.C. Winkelmann, W.F. Buhl, Y.J. Huang, C.O. Pedersen, R.K. Strand, R.J. Liesen, D.E. Fisher, M.J. Witte, EnergyPlus: creating a new-generation building energy simulation program, Energ. Buildings 33 (4) (2001) 319–331.

[22] D. Herron, G. Walton, L. Lawrie, Building Loads Analysis and System Thermodynamics (BLAST) Program Users Manual. Volume One. Supplement (Version 3.0), in, CONSTRUCTION ENGINEERING RESEARCH LAB (ARMY) CHAMPAIGN IL, 1981.

[23] P. Strachan, G. Kokogiannakis, I. Macdonald, History and development of validation with the ESP-r simulation program, Build. Environ. 43 (4) (2008) 601–609.

[24] J.A. Clarke, J.L.M. Hensen, Integrated building performance simulation: Progress, prospects and requirements, Build. Environ. 91 (2015) 294–306.

[25] D.B. Crawley, J.W. Hand, M. Kummert, B.T. Griffith, Contrasting the capabilities of building energy performance simulation programs, Build. Environ. 43 (4) (2008) 661–673.

[26] R. American Society of Heating, I. Air-Conditioning Engineers, 2021 ASHRAE® Handbook - Fundamentals (SI Edition), in, American Society of Heating, Refrigerating and Air-Conditioning Engineers, Inc. (ASHRAE), 2021.

[27] G.N. Walton, Thermal analysis research program reference manual, (No Title), (1983).

[28] D.E. Fisher, C.O. Pedersen, Convective Heat Transfer in Building Energy and Thermal Load Calculations, American Society of Heating, Refrigerating and Air-Conditioning Engineers, 1997.

[29] I. Beausoleil-Morrison, The adaptive simulation of convective heat transfer at internal building surfaces, Build. Environ. 37 (8) (2002) 791–806.

[30] F. Alamdari, G.P. Hammond, Improved data correlations for buoyancy-driven convection in rooms, Build. Serv. Eng. Res. Technol. 4 (3) (1983) 106–112.

[31] A.-J.-N. Khalifa, Heat Transfer Processes in Buildings, University of Wales, College of Cardiff, 1989.

[32] H.B. Awbi, A. Hatton, Natural convection from heated room surfaces, Energ. Build. 30 (3) (1999) 233–244.

[33] D.E. Fisher, An Experimental Investigation of Mixed Convection Heat Transfer in a Rectangular Enclosure, University of Illinois at Urbana-Champaign, 1995.

[34] Standard Practice for Estimation of Heat Gain or Loss Through Ceilings Under Attics Containing Radiant Barriers by Use of a Computer Program, ASTM International.

[35] A.D. Fontanini, J.L. Castro Aguilar, M.S. Mitchell, J. Kosny, N. Merket, J. W. DeGraw, E. Lee, Predicting the performance of radiant technologies in attics: Reducing the discrepancies between attic specific and whole-building energy models, Energ. Build. 169 (2018) 69–83.

[36] M. Camci, Y. Karakoyun, O. Acikgoz, A.S. Dalkilic, A comparative study on convective heat transfer in indoor applications, Energ. Build. 242 (2021).

[37] I. Beausoleil-Morrison, P. Strachan, On the significance of modeling internal surface convection in dynamic whole-building simulation programs, ASHRAE Trans. 105 (1999) 929.

[38] S. Obyn, G. van Moeseke, Variability and impact of internal surfaces convective heat transfer coefficients in the thermal evaluation of office buildings, Appl. Therm. Eng. 87 (2015) 258–272.

[39] L. Peeters, I. Beausoleil-Morrison, A. Novoselac, Internal convective heat transfer modeling: Critical review and discussion of experimentally derived correlations, Energ. Build. 43 (9) (2011) 2227–2239.

[40] E. Altmayer, A. Gadgil, F.S. Bauman, R.C. Kammerud, Correlation for convective heat transfer from room surfaces, ASHRAE Trans. 89 (2) (1983) 61–77.

[41] A. Rincón-Casado, F.J. Sánchez de la Flor, E. Chacón Vera, J. Sánchez Ramos, New natural convection heat transfer correlations in enclosures for building performance simulation, Eng. Appl. Comput. Fluid Mech. 11 (1) (2017) 340–356.

[42] D.J. Watson, Comparative physiological studies on the growth of field crops: I. Variation in Net Assimilation Rate and Leaf Area between Species and Varieties, and within and between years, Ann. Bot. 11 (41) (1947) 41–76.

[43] B.E. Launder, D.B. Spalding, The numerical computation of turbulent flows, Comput. Methods Appl. Mech. Eng. 3 (2) (1974) 269–289.

[44] G. Larochelle Martin, D. Monfet, High-density controlled environment agriculture (CEA-HD) air distribution optimization using computational fluid dynamics (CFD), Eng. Appl. Comput. Fluid Mech. 18 (1) (2024) 2297027.

[45] O.A. Monje, Predicting Transpiration Rates of Hydroponically Grown Plant Communities in Controlled Environments, Utah State University, 1998.

[46] S. Pantankar, D. Spalding, A calculation procedure for heat, mass and momentum transfer in three-dimensional parabolic flows, Int. J. Heat Mass Transfer 15 (1972) 1787–1806.

[47] A. Rincón-Casado, F.J. Sánchez de la Flor, 3D internal forced convection heat-transfer correlations from CFD for building performance simulation, Eng. Appl. Comput. Fluid Mech. 12 (1) (2018) 553–566.